Author/s:
Meikle, TG;Keizer, DW;Separovic, F;Yao, S

Title:
Insights into dynamic properties of water in lipidic cubic phases by 2D nuclear Overhauser effect (NOE) NMR spectroscopy

Date:
2024-07-15

Citation:
Meikle, T. G., Keizer, D. W., Separovic, F. & Yao, S. (2024). Insights into dynamic properties of water in lipidic cubic phases by 2D nuclear Overhauser effect (NOE) NMR spectroscopy. Journal of Colloid and Interface Science, 666, pp.659-669. https://doi.org/10.1016/j.jcis.2024.04.054.

Persistent Link:
https://hdl.handle.net/11343/344711

Journal of Colloid and Interface Science 666 (2024) 659–669

Contents lists available at ScienceDirect

Journal of Colloid And Interface Science

journal homepage: www.elsevier.com/locate/jcis

Regular Article

Insights into dynamic properties of water in lipidic cubic phases by 2D nuclear Overhauser effect (NOE) NMR spectroscopy

Thomas G. Meikle [a], David W. Keizer [b], Frances Separovic [b,c], Shenggen Yao [b,*]

[a] Baker Heart and Diabetes Institute, Melbourne, VIC 3004, Australia
[b] Bio21 Molecular Science and Biotechnology Institute, The University of Melbourne, VIC 3010, Australia
[c] School of Chemistry, The University of Melbourne, VIC 3010, Australia

GRAPHICAL ABSTRACT

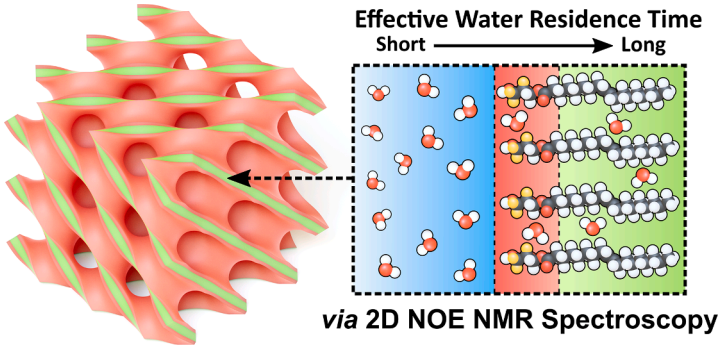

ARTICLE INFO

Keywords:
Cross-relaxation
Dynamic properties of water
Lipidic cubic phases
Nuclear magnetic resonance
Nuclear Overhauser effect

ABSTRACT

Two-dimensional NOE (nuclear Overhauser effect) NMR spectroscopy was employed to investigate the dynamic properties of water within lyotropic bicontinuous lipidic cubic phases (LCPs) formed by monoolein (MO). Experiments observed categorically different effective residence times of water molecules: (i) in proximity to the glycerol moiety of MO, and (ii) adjacent to the hydrophobic chain towards the hydrocarbon tail of MO, as evidenced by the opposite signs of intermolecular NOE cross peaks between protons of water and those of MO in 2D ^{1}H–^{1}H NOESY spectra. Spectroscopic data delineating the different effective residence times of water molecules within both the gyroid (Q_{II}^{G}) and diamond (Q_{II}^{D}) phase groups corresponding to hydration levels of 35 and 40 wt%, respectively, are presented. Additionally, an increase in effective residence time of water molecules in proximity to the glycerol moiety of MO in LCPs was observed upon storage at ambient temperature and in the presence of an additive lipid, cholesterol. Atom-specific NOE build-up curves for protons of water and those of MO are also given. The results presented herein provide new insight into the physicochemical properties and behaviour of water in LCPs, and demonstrate an additional avenue for experimental study of water–lipid interactions and hydration dynamics in model membranes and nanomaterials using 2D NOE NMR spectroscopy.

* Corresponding author at: Bio21 Molecular Science and Biotechnology Institute, The University of Melbourne Victoria 3010 Australia.
E-mail address: shyao@unimelb.edu.au (S. Yao).

https://doi.org/10.1016/j.jcis.2024.04.054
Received 25 January 2024; Received in revised form 3 April 2024; Accepted 8 April 2024
Available online 9 April 2024

1. Introduction

In molecular self-assemblies, the dynamic properties of water molecules are considered critical in understanding their biological activity and behaviour [1,2]. A variety of spectroscopic methods, including fluorescence [3], infrared [4], neutron scattering [5], and Raman scattering [6], have sporadically been used to study the properties of hydration water in lipid self-assemblies, including lipidic cubic phases (LCPs).

LCPs are formed *via* the spontaneous self-assembly of certain lipids in an aqueous environment and have found a range of applications, including as lipid-based membrane mimetics in the crystallization of integral membrane proteins for structure determination by X-ray crystallography;[7,8] and as potential matrices for drug and nutrient delivery/release *in vivo* [9–11]. LCPs are comprised of a single lipid bilayer contorted in three-dimensional (3D) space such that their geometry approximates that of a triply periodic minimal surface, featuring two interpenetrating but unconnected networks of water channels. A 3D illustration of a diamond phase $\left(Q_{II}^{D}\right)$ LCP and a schematic cross-sectional view are shown in Fig. 1.

Previously, the ultrafast dynamics of the water of hydration in LCPs have been probed using time-resolved fluorescence spectroscopy, following the incorporation of a series of tryptophan alkyl ester probes into the lipid bilayer. Three distinct temporal scales of water molecules were identified based on their proximity to lipid molecules [3]. Recently, a comprehensive study by Fourier-transform infrared spectroscopy (FTIR) and broadband dielectric spectroscopy (BDS) of water state during LCP phase transitions over a range of temperatures has been reported [12]. Molecular dynamic simulations have also been used to demonstrate the role of nanoconfinement and hydration dynamics in the crystallization of small molecules encapsulated within LCPs [13].

The nuclear Overhauser effect (NOE), arising from spin-spin cross-relaxation in NMR, has long been used to study intra- and intermolecular contacts, including solvent exposure and protein hydration dynamics [14,15]. In addition to its indispensable role in the structural elucidation of macromolecules by NMR, 2D ^{1}H–^{1}H homonuclear NOE spectroscopy (NOESY) has been used to probe the molecular disorder of lipid headgroups and hydrocarbon chains [16,17], and molecular interactions between dendrimers and surfactants [18]. 2D ^{1}H-^{19}F/^{7}Li heteronuclear NOE spectroscopy (HOESY) has also been employed to gain insight into inter-ionic interactions in ionic liquids [19,20]. Furthermore, magic angle spinning (MAS) NOESY with the application of pulsed field gradients has been used to study the interaction of water with 1-palmitoyl-2-oleoyl-glycerol-3-phosphocholine bilayers in the fluid phase [21]. Notably, the observation of interactions between the protons of water molecules and the non-exchangeable protons of the MO glycerol moiety in LCPs, detected via MAS 2D ^{1}H–^{1}H ROESY (NOE in the rotating frame), has been reported previously [22]. Recently, intermolecular interactions in phytantriol-based lyotropic liquid crystals detected by 2D ^{1}H–^{1}H NOESY spectra have also been reported [23].

In the present study, 2D ^{1}H–^{1}H NOESY spectra were used to explore the dynamic properties of water in LCPs formed by MO. Initially, we present experimental evidence of categorically different effective residence times of water molecules in proximity to the glycerol moiety of MO and those in the region adjacent to the hydrocarbon chain of MO. Secondly, we report experimental observation of an increase in the effective residence time for water molecules in the proximity of the glycerol moiety of MO in LCPs over time and in the presence of an additive lipid, cholesterol, at 20 mol% lipid content. Finally, cross-relaxation rates for water and non-exchangeable protons of MO in LCPs, obtained from NOE build-up curves, are also included.

The results presented herein provide new insight into the physicochemical properties of water molecules in LCPs and demonstrate an additional avenue for the study of water–lipid interactions and hydration dynamics in lipid self-assemblies and nanomaterials using 2D NOE NMR spectroscopy. They are of particular relevance for the study of membrane proteins in LCP systems. Measured changes in the residence times of water suggest alteration to the hydration shell at the lipid-water interface, with implications for the stability and activity of encapsulated proteins. Furthermore, the hydration dynamics of LCPs and similar nanomaterials can be expected to play a role in the diffusion and release of small molecules, highlighting the importance of understanding these processes for the design of drug encapsulation and release matrices [24].

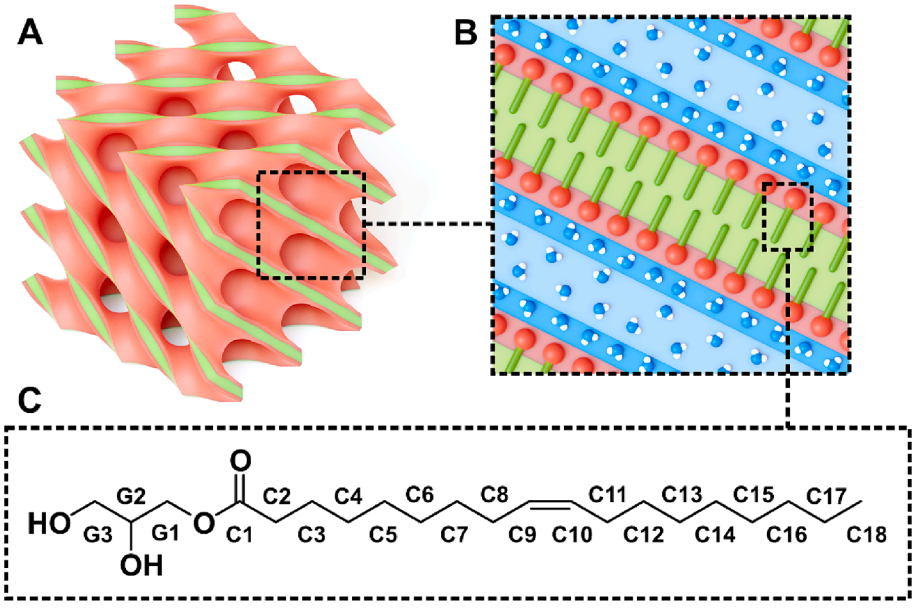

Fig. 1. A 3D illustration of the diamond phase $\left(Q_{II}^{D}\right)$ LCP – showing (A) only the lipid bilayer, with the headgroup region coloured red and the hydrophobic tail region coloured green, and (B) a schematic view of the cross section of LCPs highlighting both the lipid bilayer and water channel. (C) The chemical structure of monoolein (MO) is depicted with atom names indicated based on their corresponding carbon positions.

2. Materials, theory and methods

2.1. Sample preparation

Monoolein (MO, ≥99 %) and cholesterol (≥99 %) were purchased from Sigma-Aldrich (St Louis, MO). Chloroform-D ($CDCl_3$, 99.8 %) was purchased from Cambridge Isotope Laboratories (Tewksbury, MA). LCP samples were prepared by mixing 10 mM HEPES buffer solution, pH 7.0, with molten MO (with or without cholesterol) using a coupled syringe apparatus as detailed previously [25]. A capillary containing the LCP was flame sealed and then placed into a standard 5 mm NMR tube filled with $CDCl_3$, used to lock the magnetic field. Freshly prepared LCP samples were allowed to equilibrate for approximately 12 h prior to their first NMR measurements, and stored at 18–22 °C for future experiments.

2.2. NMR measurement and spectral analysis

All NMR spectra were acquired at 298 K on a Bruker AvanceIII 600 spectrometer, equipped with a Bruker TCI cryoprobe fitted with a single-axis field gradient (*Gz*). Spectral data were subsequently processed and analysed using TOPSPIN (Version 3.6, Bruker) with ^{1}H chemical shifts referenced to that of residual $CHCl_3$ in $CDCl_3$ at 7.24 ppm. Standard 2D NOESY and ROESY pulse sequences (*noesygpphpp* and *roesyphpp*, Bruker pulse sequence library) were used for spectral acquisition. All 2D spectra were acquired with 1024 by 256 complex data points and a recycle relaxation delay of 2.0 s. The datasets were linear predicted to 512 complex points in the indirect (F1) dimension and phase-shifted sine-bell window functions were applied for both dimensions before Fourier transformation (FT). The final data matrix after FT was 1024 by 1024. For the determination of cross-relaxation rates between protons of water molecules and those of MO, a series of 2D NOESY spectra with mixing times ranging from 50 ms to 1.2 s were acquired for MO LCPs at a hydration of 35 wt%. Before the integration of individual cross peaks in 2D NOESY, reduction of t1 noise for all 2D NOESY spectra were carried out via subtracting each row of the 2D NOESY spectrum from the projection of a sub-spectral region containing only the noise ridges [26,27]. The analysis of inter-molecular cross-relaxation rates was carried out in SigmaPlot (SPSS Inc., Version 12.5).

2.3. Spin-spin cross-relaxation in the laboratory and rotating frames – dependence of the correlation time on intermolecular interactions

In contrast to 2D ROESY spectra, where cross peaks arising from cross-relaxation are always in opposite phase in relation to the diagonal peaks, the relative phase of intramolecular cross peaks in 2D NOESY spectra depends on the overall rotational correlation time of the molecule containing the pair of spins under consideration. At a given field strength (Larmor frequency ω_0), in general, for small molecules with fast rotational correlation times, τ_c, ($\omega_0\tau_c \ll 1$), NOE cross peaks in 2D NOESY spectra appear in opposite phase to the diagonal peaks, whereas for large molecules with slow rotational correlation times, τ_c, ($\omega_0\tau_c \gg 1$), NOE cross peaks are in the same phase as the diagonals. A sign change of cross-peaks in NOESY then occurs at $\omega_0\tau_c = \frac{\sqrt{5}}{2}$, corresponding to τ_c of 300 ps at a spectrometer frequency of $\omega_0 = 2\pi \times 600$ MHz. The same is true for intermolecular cross-relaxation where both signs of the intermolecular cross peaks in relation to the diagonals may be observed in 2D NOESY depending on the timescales of motion of the pair of spins involved [28]. Depending on the model used for the description of the length and orientation of the vector between the two spins involved in the dipole–dipole interaction, such as the rigid sphere model, the explicit forms of the spectral density function for the intermolecular cross-relaxation may vary. In the present context, a spectral density function given below is utilized to account for three distinct types of motions: (1) the fast vibrational and re-orientational motions of the water protons and protons of lipid molecules with which the water interacts, (2) diffusion-based water protons into and out of the hydration site, and (3) the overall tumbling time of the lipid/water system [29].

$$J(w) = \left[\frac{(1-S^2)\tau_f}{1+(\omega\tau_f)^2} + \frac{S^2\tau_d}{1+(\omega\tau_d)^2}\right] \quad (1)$$

where S^2 is the order parameter, a measure of the flexibility of the fast timescale motion of the vector between the two spins involved under consideration, ranging from 0 to 1 for complete disorder and completely rigid, respectively. τ_f and τ_d are the effective correlation times of fast and slow motion, respectively, and are defined by:[29,30]

$$\tau_f = \left[\frac{1}{\tau_{res}} + \frac{1}{\tau_{fast}}\right]^{-1} \quad (2)$$

$$\tau_d = \left[\frac{1}{\tau_{res}} + \frac{1}{\tau_c}\right]^{-1} \quad (3)$$

where τ_{res} is termed the residence time of the water molecules, a measure of the diffusion of water molecules into and out of the hydration layer, with an averaged residence time of water being inversely proportional to the sum of the lateral/translational diffusion coefficients of lipids and water [30]. τ_{fast} and τ_c are the fast timescale correlation time of the pair of spins and the overall rotational re-orientational time of the lipid molecules (macromolecules), respectively. In the simplest model that the water at the hydration site is rigidly bound to the lipid molecules ($S^2 = 1$), the first term on the right side of Eq. (1) vanishes and the spectral density function is dominated by the remaining correlation time of τ_d (Eq. (3)).[30]

The cross-relaxation rates in the laboratory frame, σ^{NOE}, and in the rotating frame, σ^{ROE}, between two protons as a function of the spectral density function given in Eq. (1) are then expressed by:[30,31]

$$\sigma^{NOE} = q[6J(2\omega) - J(0)] \quad (4)$$

$$\sigma^{ROE} = q[3J(\omega) + 2J(0)] \quad (5)$$

where $q = \frac{1}{10}\hbar^2\gamma^4\left(\frac{\mu_0}{4\pi}\right)^2\left(\frac{1}{r^6}\right)$, $\gamma$is the gyromagnetic ratio of protons, $\hbar$ is the reduced Planck's constant (h/2π), μ_0 is the magnetic permeability in vacuum, and r is the interproton distance.

A plot of cross-relaxation rates of σ^{NOE} and σ^{ROE} as a function of water residence time, τ_{res} calculated using Eqs. (4) & (5), is shown in Fig. 2. Here, a change of signs for the cross peaks in the NOESY spectra occurs at the water residence time of approximately 380 ps with the parameters used in the calculations.

2.4. Cross-relaxation build-up curves for 2D NOESY

Quantitative analysis of spin cross-relaxation rate (absolute value) for gaining insight into spatial distance/contacts between spins involved is commonly carried out under the assumption of two isolated spins, i.e., potential spin–spin coupling effects are considered negligible. The (sign-sensitive) intensities of cross peaks in 2D NOESY spectra as a function of mixing time, τ_m, i.e., the NOE build up curve, is then described by: [28,31,32]

$$NOE(\tau_m) = \frac{a_{AB}(\tau_m)}{a_{AA}(0)} = \pm\left(\frac{\sigma}{R_C}\right)\exp(-R_L\tau_m)[1-\exp(-R_C\tau_m)] \quad (6)$$

with the corresponding diagonal or auto-correlations peaks given by:

$$\frac{a_{AA}(\tau_m)}{a_{AA}(0)} = \frac{1}{2}\exp\left[-\left(R-\sigma\right)\tau_m\right][1+\exp(-2\sigma\tau_m)] \quad (7)$$

where the cross-relaxation rate constant R_C and the leakage relaxation rate constant R_L are defined by $R_C = \left[(R_{AA}-R_{BB})^2 + 4\sigma^2\right]^{\frac{1}{2}}$ and $R_L =$

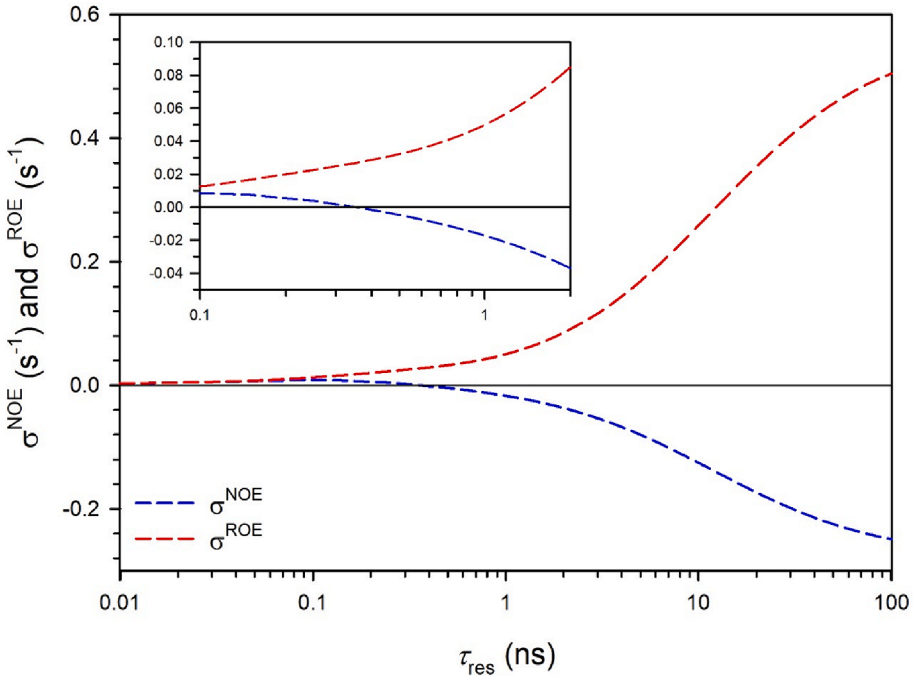

Fig. 2. Cross-relaxation rates, σ^{NOE} (blue) and σ^{ROE} (red), as a function of water residence time, τ_{res}, on the surface of the host (protein or lipid) molecules calculated using Eqs. (4) & (5) with the following parameters: $\tau_{fast} = 10$ ps, $\tau_c = 12$ ns, $S^2 = 0.3$, r = 3.0 Å, and ^{1}H frequency of 600 MHz. The inset shows an expanded view of the changeover of the sign of σ^{NOE} at the water residence time of approximately 380 ps for the parameters used. A change of fast timescale of motion, e.g. a shortening of τ_{fast} and/or an increase in S^2 in Eq. (1) will lead to a shift of the change of the sign of σ^{NOE} towards the left side of the horizontal axis. In other words, it results in an apparent increase in the effective residence time of water.

$\frac{1}{2}[(R_{AA} + R_{BB}) - R_C]$, respectively. R_{AA} and R_{BB} are spin–lattice relaxation rates of spin A and B, respectively [28,31]. It is worth noting that a simplified form of Eq. (6) assuming both spins in the two-spin system having identical spin–lattice relaxation rates, i.e., $R_{AA} = R_{BB} = R$, has also been used in the analysis of NOE cross-relaxation. By substituting $R_C = 2\sigma$ ($\sigma > 0$) and $R_L = (R - \sigma)$ into Eq. (6), we have:[19,33]

$$NOE(\tau_m) = \frac{a_{AB}(\tau_m)}{a_{AA}(0)} = \pm\frac{1}{2}\exp[-(R-\sigma)\tau_m][1 - \exp(-2\sigma\tau_m)] \quad (8)$$

Similarly, for the analysis of intermolecular cross-relaxation, including both homo- and hetero-nuclear cross-relaxation, both the simplest version Eq. (8) [34] and the original form Eq. (6), accounting for individual relaxation rates of both spins, have been applied in previous studies [19]. In the present study, fitting of cross-relaxation build-up curves with Eq. (6) was attempted first, but a satisfactory fitting parameter did not converge for R_C throughout for individual hydrogens of MO. It has been noted previously that errors of fitting for R_C tended to be high due to multiple parameter dependence and competing pathways of magnetization transfer when all three parameters, i.e., σ, R_C and R_L were iterated in the regression [28]. Subsequently, the reduced form of Eq. (8) was used in the analysis of build-up curves of cross-relaxation rates between protons of water and those of lipids in LCPs formed by MO at a hydration of 35 wt%.

3. Results and discussion

3.1. 2D NOESY and ROESY spectra of LCPs formed by MO

A pair of 2D NOESY and ROESY spectra of LCPs of phase Q_{II}^D formed by MO at a hydration of 40 wt% is given in Fig. 3. As expected, we observed not only NOE cross peaks between protons along the hydrocarbon chain of MO, but also strong cross peaks between the water and hydroxyl groups of the MO glycerol moiety. The latter indicate the presence of chemical exchange between the MO hydroxyl groups and the water of hydration.

The relative phase of the cross peaks arising from intramolecular cross-relaxation are in phase with those of the diagonal peaks, indicating that $\omega_0\tau_c \gg 1$, and thus the MO molecules in the LCP can be said to behave similarly to macromolecules. This is expected given the tightly ordered structure of lipids in the LCP. Also presented in Fig. 3 are cross peaks arising from intermolecular cross-relaxation between water and the non-exchangeable protons along the MO hydrocarbon chain, including those between protons of water molecules and non-exchangeable hydrocarbon attached protons, such as G1, G2, and G3 in the glycerol moiety of MO, which have been previously reported using MAS 2D ^{1}H–^{1}H ROESY [22].

A close examination of the 2D NOESY reveals that cross peaks between water and G2/G3 are in opposite phase to the majority of those observed between water and non-exchangeable protons of MO along the hydrocarbon chain, such as G1, *C*2, C3, etc. (Fig. 3A). The corresponding cross peaks between water and G2/G3 in the ROESY spectrum are unfortunately dominated by the cross peaks arising from the chemical exchange between the neighbouring hydroxyl groups, G2-OH/G3-OH, and water via the TOCSY mechanism during spinlock, which always appear in the same phase as the diagonals (Fig. 3B).

3.2. Two categorically different effective residence times of water molecules in LCPs formed by MO

The observation that the cross peaks between water and G2/G3 are opposite in phase to the majority of cross peaks between water and non-exchangeable protons along the entire MO hydrocarbon chain indicates the presence of two categorically different effective residence times of water molecules: one for those in proximity to the glycerol moiety of MO, and another for those in proximity to the hydrocarbon chain. The finding of two categorically different effective residence times of water molecules in MO-based LCPs, as shown in Fig. 3, was then replicated in an LCP sample of the phase group Q_{II}^G formed by MO at a hydration of 35 wt%. A detailed study of intermolecular cross-relaxation between

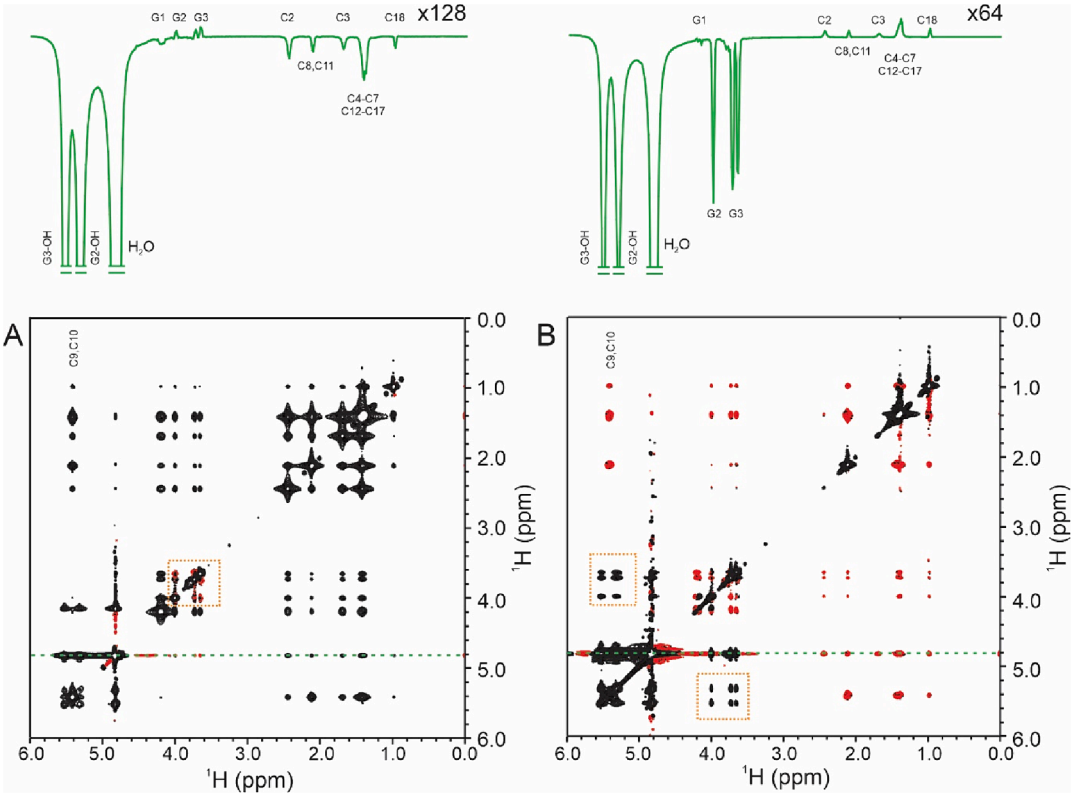

Fig. 3. Phase sensitive 2D NOESY and ROESY spectra of LCPs formed by MO at a hydration of 40 wt%. (A) 2D NOESY spectrum where the majority of cross peaks arising from cross relaxation and those from chemical exchange are negative in phase (black) in relation to the diagonals, except intermolecular cross peaks between water and G2/G3, which are positive in phase (red). DQF-COSY type of anti-phase cross peaks between G2 and G3 in the NOESY spectrum (highlighted by orange dashed box) originate from zero-quantum artefact commonly seen in NOESY spectra; (B) 2D ROESY where cross peaks arising from cross-relaxation (positive in phase and shown in red) appeared in opposite phase to diagonal peaks and those arising from chemical exchange/TOCSY are in the same phase as diagonals (negative in phase and shown in black). Additional cross peaks seen between G1/G2/G3 and G2-OH/G3-OH (highlighted by orange dashed box) arise from TOCSY/exchange transfer commonly seen in ROESY spectra. Shown above the corresponding 2D spectra are 1D slices across the water resonance along the F1 dimension after scaling up as indicated (green dashed lines). Both 2D NOESY and ROESY spectra were acquired with a mixing time of 300 ms.

protons of water and those along the entire MO hydrocarbon chain, via acquiring a series of NOE spectra at different mixing times, was then carried out for the Q_{II}^{G} LCP (MO at 35 wt% H_2O) and the outcome is summarized in Fig. 4.

The stack plot of 1D slices across the water resonance along the F1 dimension of 2D NOESY spectra acquired with mixing times ranging from 60 to 750 ms (Fig. 4C) unequivocally confirms the presence of two groups of cross-relaxation peaks, where those arising between water and G2/G3 are in opposite phase to the majority of cross peaks between water and non-exchangeable protons along the lipid hydrocarbon tail. Based on the NOE dependence on the residence time of water, as shown in Fig. 2, the 2D NOESY spectra confirm two groups of residence times for water molecules in the proximity of MO LCPs. This experimental result indicates a comparatively fast residence time for water in proximity to G2/G3, and is consistent with the location of these spins in close proximity to the water channel, in contrast to that of the hydrocarbon chain of MO towards its hydrophobic tail (Fig. 1). It is worth noting that a change in sign of the cross peaks, normally as a result of contribution from relayed magnetization transfer at longer mixing time [21], was not observed.

These observations are likely reflective of the fundamentally distinct chemical environments found at different points across the lipid bilayer and the hydration gradient that occurs. The polar nature of the lipid headgroups and the high degree of hydration appear conducive to shorter residence times, wherein water molecules can rapidly exchange with bulk water within the channels of the LCP. In contrast, water has little affinity for the bilayer hydrophobic core, and this region experiences a lower degree of hydration. Water is present here as defects in lipid organization, and the steric constraints imposed by the packed hydrocarbon chains could result in an apparent longer residence time.

3.3. Change of effective residence time of water in proximity to G2/G3 over time

1D ^{1}H spectra of LCPs formed by MO have been reported previously, with notable spectral variations occurring over time [25]. As the sample aged, the hydroxyl resonances of the glycerol moiety of MO gradually dissipated together with an increase in linewidth for the water resonance. This observation is consistent with a change in exchange kinetics between the MO hydroxyl groups and water, i.e., a shift from a slow to an intermediate exchange regime on the NMR chemical shift scale over time.

Here, we report a new feature of LCPs with time as revealed by 2D NOESY spectra, where an increase in effective residence time for water in the proximity of G2/G3 is clearly evident, as can be readily identified by the relative phase of their corresponding cross peaks with water. Fig. 5 shows a pair of 2D NOESY and ROESY spectra of LCPs formed by MO at a hydration of 40 wt%. Spectra were acquired after the sample was stored for approximately 2.5 months at 18–22 °C. Note that the cross peaks arising from the chemical exchange between water and hydroxyl groups, G2-OH/G3-OH, of glycerol in MO, which are clearly present in Fig. 3, are barely visible in Fig. 5 due to line broadening. Again, this observation is characteristic of intermediate exchange on the NMR chemical shift timescale. Accordingly, the influence of the corresponding chemical exchange on cross peaks between water and G2/G3 in the ROESY spectrum was significantly reduced (Fig. 5B) in

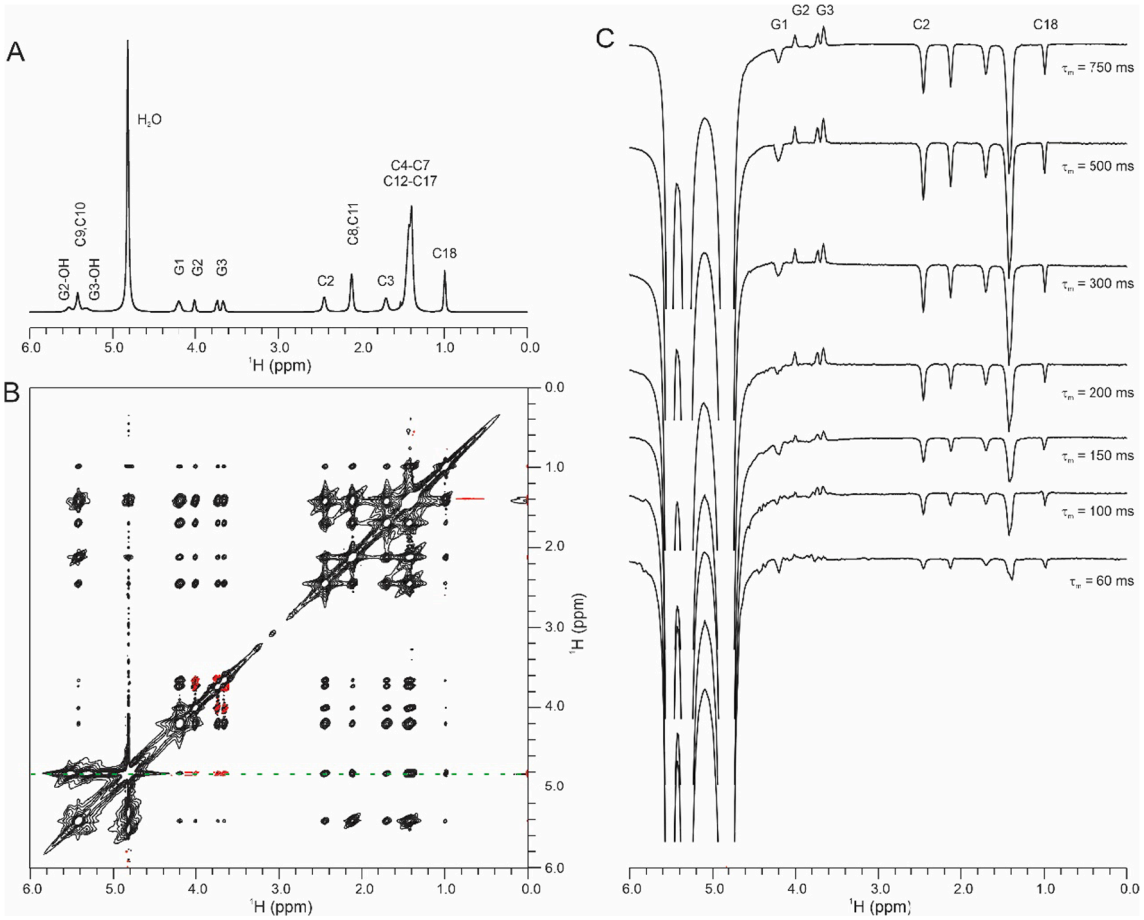

Fig. 4. Different categorical residence times observed experimentally by 2D NOESY for water molecules near the glycerol head group and those in proximity to the hydrocarbon chain, in a Q_{II}^{G} LCP sample comprised of MO at 35 wt% H_2O. (A) 1D ^{1}H spectrum of LCPs with resonances labelled based on their corresponding carbon atoms; (B) 2D phase sensitive NOESY acquired with a mixing time of 300 ms. Cross peaks between water and G2/G3 are in opposite phase compared to those between water and other non-exchangeable protons along the hydrocarbon chain of MO; (C) Stack plot of 1D slices across the water resonance along the F1 dimension in 2D NOESY (green dashed lines in B) over a series of mixing times, where cross peaks arising from cross-relaxation between water and G2/G3 are in opposite phase to those between water and other non-exchangeable protons along the hydrocarbon chain of MO for the entire range of mixing times of the NOESY spectra recorded.

comparison to the corresponding ROESY spectrum shown in Fig. 3B.

Based on Fig. 2 and Eqs (1)–(5), several factors may be responsible for the observed change in effective residence times of water in the proximity of G2 and G3 with sample age. Notably, the chemical stability of the sample is confirmed as no chemical modification of MO is detected over this time. Furthermore, judging from the 1D ^{1}H spectra, the isotropic nature of the sample remains, otherwise significant peak broadening would be evident [25]. While small angle X-ray scattering (SAXS) data was not collected at the 2.5 month timepoint, the effective residence time of water in this sample differs from both non-aged Q_{II}^{G} (35 % H_2O) and Q_{II}^{D} (40 % H_2O) LCP samples, and so this effect is unlikely explained simply by a change in LCP phase group alone.

Given the lack of significant change in the translational diffusion coefficients of either lipid or water during this time, which would suggest a direct increase in τ_{res}, the observed increase in the effective residence time of water likely stems from a reduced fast motion associated with the spins of lipid and water groups. This is suggestive of changes in local dynamics, rather than overall molecular motions.

One possible mechanistic explanation for this observation of increased effective residence time of water proximal to G2 and G3 involves change in the ordering or packing of lipid molecules over time. States of metastability or long-lived non-equilibrium states have previously been observed in LCP samples [35,36], and thus changes in lipid order may occur well beyond the 12 h period of equilibration used for initial samples. Reordering of lipids across large timescales may promote more stable or extensive hydrogen-bonding networks, increasing effective residence time of water molecules near G2/G3.

3.4. *Increase of effective residence time of water in proximity to G2/G3 in the presence of cholesterol*

The 1D ^{1}H spectra of an LCP formed by MO at hydration of 40 wt%, in the absence and presence of 20 mol% cholesterol, are given in Fig. 6. Using SAXS, addition of cholesterol was observed to induce a phase transition from Q_{II}^{D} to Q_{II}^{G}. Like its 1D ^{13}C counterpart previously reported [25], the 1D ^{1}H spectrum of a LCP in the presence of cholesterol remains dominated by signals from MO with a very minor overall upfield shift visible (indicated by dashed red lines, Fig. 6B). Also shown in Fig. 6 is a 2D NOESY spectrum of MO LCP with cholesterol, where cross peaks between water and G2/G3 are in the same phase as those between water and other non-exchangeable protons along the MO hydrocarbon chain. This phase change for NOE cross peaks between water and G2/G3 in the presence of cholesterol likely indicates an increase in the effective residence time of water in proximity to G2/G3.

A possible explanation for the slowdown in residence time of water in proximity to G2/G3 in the presence of cholesterol is likely related to an alteration in hydrogen bond formation between water, cholesterol, and MO [37]. While the translational diffusion of water largely remains unchanged, a decrease in lipid translational diffusion in the presence of cholesterol in LCPs formed by MO has been reported [38,39]. This

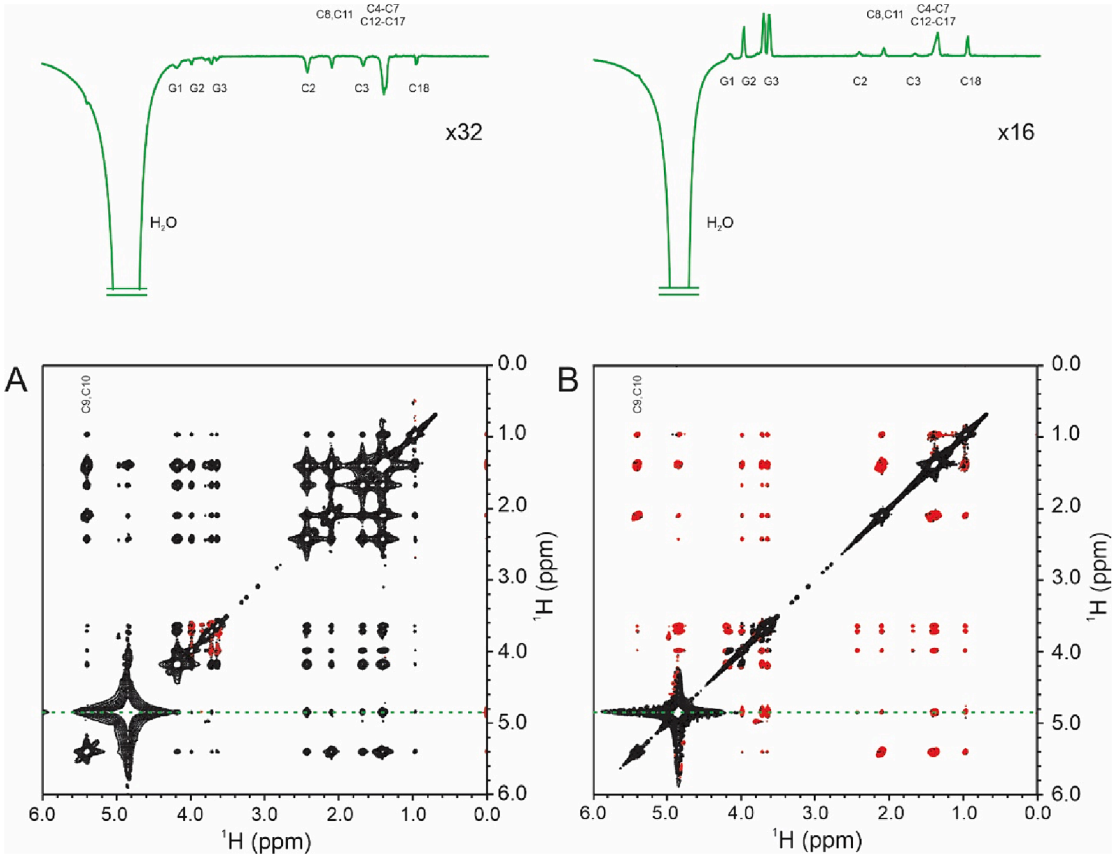

Fig. 5. NMR evidence of an increase in residence time of water in proximity to G2/G3 over time in LCPs: (A) Phase sensitive 2D NOESY, and (B) 2D ROESY of LCPs, formed by MO at a hydration of 40 wt%, acquired approximately two and a half months after sample preparation. The sample was stored at ambient temperature during this time. Similar to Fig. 3 presented above, the 2D NOESY and ROESY spectra are 1D slices across the water resonance along the F1 dimension (marked by the dashed line in green) where a phase change for cross peaks between water and G2/G3 is clearly evident compared to that shown in Fig. 3.

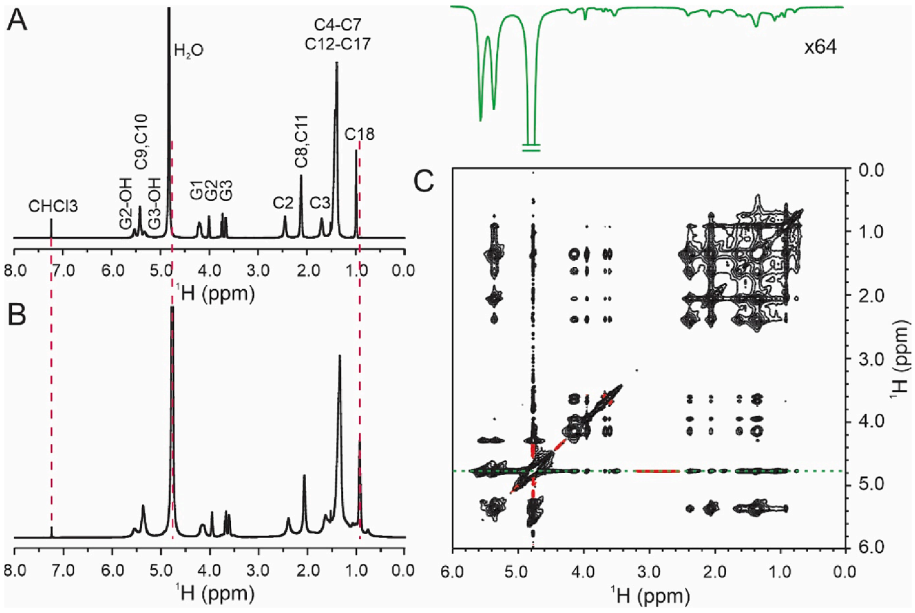

Fig. 6. NMR evidence of an increase in residence time of water in proximity to G2/G3 due to the presence of cholesterol in LCPs formed by MO. 1D ^{1}H spectrum of LCPs of MO at a hydration of 40 wt%: (A) in the absence of cholesterol, and (B) in the presence of 20 mol% cholesterol. (C) 2D phase sensitive NOESY acquired with a mixing time of 300 ms. Shown above the 2D NOESY spectrum is the 1D slice across the water resonance along the F1 dimension after scaling up as indicated (green dashed lines).

suggests a possible source for an increase in τ_{res} as the averaged residence time of water is inversely proportional to the sum of the translational diffusion coefficients of lipids and water [30]. The influence of cholesterol on hydration water in lipid membranes is of great interest, though there has been limited experimental data reported [40]. Based primarily on molecular dynamics simulation and some pioneering experimental results from Overhauser dynamic nuclear polarization (DNP) relaxometry[40] and FTIR [41], an increase in bulk-like water in proximity to the interfacial region of lipid membranes in the presence of cholesterol, and subsequently an increase of surface water diffusivity, has been proposed [41–43].

3.5. Cross-relaxation rates between protons of water and those of MO in LCPs

The build-up curves for intermolecular NOEs between protons of water and those of lipids in LCPs formed by MO at 35 wt% hydration obtained by acquiring a series of NOESY spectra are shown in Fig. 7A. The cross-relaxation rates determined by fitting the data with Eq. (8) are tabulated in Table 1 and plotted in Fig. 7B at each position along the MO

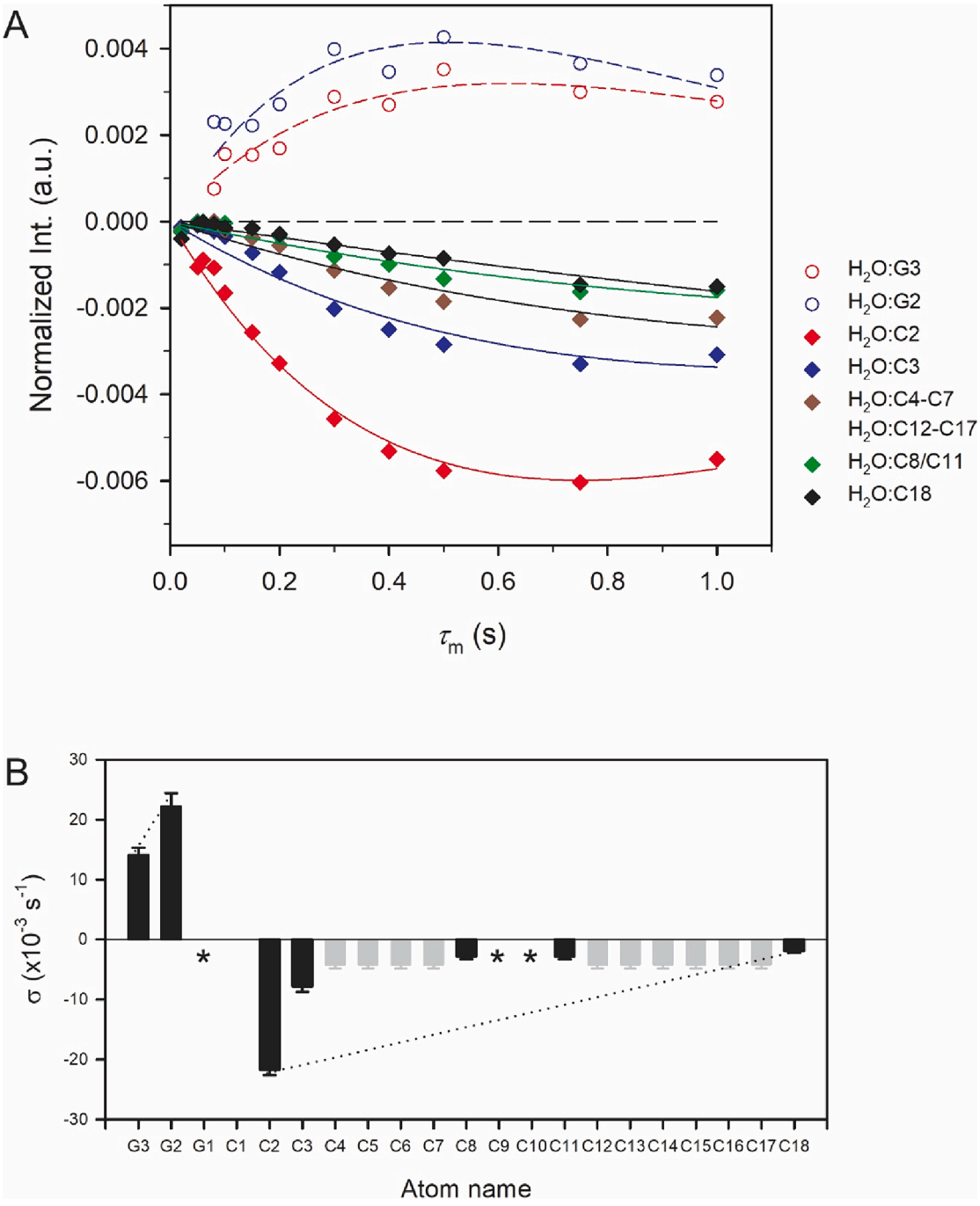

Fig. 7. Cross-relaxation rates between protons of water and those of lipids in LCPs formed by MO at a hydration of 35 wt%. (A) NOE build-up curves for protons of water and those of MO in an LCP obtained from 2D ^{1}H -^{1}H NOESY spectra (see Fig. 4). Intensities were normalised to the absolute intensities of the corresponding diagonal peaks of MO protons. Both solid and dashed lines are from the fitting of Eq. (8). (B) Experimentally determined cross-relaxation rates for individual proton pairs along the MO hydrocarbon chain. Grey bars indicate protons giving rise to degenerate ^{1}H chemical shift resonances, as a result an averaged fitting outcome is presented. An asterisk indicates measurement was not made due to spectral limitations. The dotted lines are shown to guide the eyes only.

Table 1
Cross-relaxation rates between protons of water and those of lipids in LCPs formed by MO at a hydration of 35 wt%.

Proton Pairs	σ ($\times 10^{-3}$ s^{-1})	R (s^{-1})
H_2O:G3	14.1 ± 1.2	1.62 ± 0.15
H_2O:G2	22.2 ± 2.2	1.97 ± 0.18
H_2O:G1	–	–
H_2O:C2	−21.7 ± 0.9	1.34 ± 0.07
H_2O:C3	−7.8 ± 0.9	0.84 ± 0.16
H_2O:C4-C7 H_2O:C12-C17	−4.2 ± 0.6	0.55 ± 0.19
H_2O:C9/C10	–	–
H_2O:C8/C11	−2.8 ± 0.5	0.46 ± 0.22
H_2O:C18	−1.9 ± 0.3	0.15 ± 0.23

hydrocarbon chain. Evaluation of the cross-relaxation between protons of water molecules and G1 was not attempted due to the closeness of its resonance to that of water. Elucidation of the cross-relaxation between protons of water and those of C9/C10 was hampered by the presence of nearby resonances of hydroxyl groups undergoing exchange with water. The intermolecular cross-relaxation rates along the hydrocarbon chain of MO are relatively weak (see scale of Fig. 7B). A general trend for weakening of intermolecular cross-relaxation is generally anticipated towards the hydrophobic tail of the lipid molecules as less water molecules are expected to be entrapped. In addition to hydration dynamics, including residence time and density of water molecules in proximity to the specific hydrogens of MO, the apparent variation along the MO chain could be influenced by molecular configurations and intermolecular forces.

Given the multiple parameter dependence in the fitting of the cross-relaxation rate, σ, caution is needed in the interpretation of fitted values, particularly where the signal-to-noise of the cross peaks is inadequate. For intermolecular NOEs, a decrease in mutual self-diffusion for the interacting pairs may cause a decrease in cross-relaxation rates [28].

In general, depending on the spectral properties of individual spins, quantification of intermolecular cross-relaxation for certain spins, such as G1/G2/G3, may be hampered by their closeness to the water resonance. In addition, the behaviour of neighbouring spins could hinder the quantification of cross-relaxation in certain spins of interest. For example, chemical exchange between hydroxyl groups (G2-OH and G3-OH) and water complicates the evaluation of cross-relaxation between G2/G3 and water, as well as C9/C10 and water, in both NOESY and ROESY spectra. Alternative NMR pulse sequences that better handle the water resonance than the generic version used in the present study could be explored for more optimal outcomes. For example, employing NOESY spectra with water suppression prior to acquisition, to eliminate the influence of the water resonance ridge along the F1 dimension, will allow cross-relaxation transferred from hydrocarbon chain protons to hydration water to be evaluated with minimal impact from water ridges (the broad foot of water resonance along the F2 dimension) present in the conventional NOESY spectra. Furthermore, heteronuclear Overhauser effect spectroscopy (HOESY), an analogue of NOESY, has been used to study intermolecular contacts, such as those between pairs of ^{1}H and ^{19}F or ^{1}H and ^{7}Li nuclei. This may avoid the previously mentioned limitations in ^{1}H–^{1}H NOESY spectra, depending on the identity of the lipids constituting the LCP. For MO LCPs, a ^{1}H–^{13}C HOESY experiment would benefit from selective/uniform ^{13}C-enriched MO as far as spectral sensitivity is concerned since, at natural abundance, sensitivity limitations make quantitation untenable.

Interactions between water and biomolecules, especially protein hydration dynamics, are considered to play a critical role in the function of all biological systems. Despite this, advances in the experimental quantification of such effects at the atomic level have been slow. Solution NMR has been long considered as the leading means for gaining insight into site-specific protein hydration dynamics *via* the measurement of NOEs between water and amide protons of proteins. There have been successful studies of residue-specific quantitative information about hydration water mobility obtained from intermolecular NOEs with the aid of a model that explicitly incorporates dynamic heterogeneity [44]. Additionally, quantitation measurement of water diffusion lifetimes at the protein interface has been achieved via the ratio of ROE and NOE cross-relaxation rates between water and backbone amides [29].

The presence of excessive bulk water molecules outside the hydration layer, which contribute to experimentally measured intermolecular NOE though long-range dipole–dipole coupling and chemical exchange, to a certain extent has limited the use of NOESY based methods for the study of protein hydration dynamics. More recently, quantification of site-specific protein hydration dynamics by NMR has been revisited with the introduction of protein encapsulation in reverse micelles. Encapsulation of proteins in the aqueous centre of reverse micelles effectively eliminates the excessive bulk water around the protein of interest and thus significantly reduces hydrogen exchange chemistry and considerably slows down the rapid water dynamics normally present in aqueous solutions [45–47]. It also recently has been demonstrated by NMR that elimination of excessive water molecules outside the hydration layer commonly present with macromolecules in solution similarly can be achieved by encapsulation in LCPs [48].

In the case of tryptophan dynamics measured by time-resolved fluorescence spectroscopy, the solvation dynamics of bulk water, at a timescale *ca.* 1–2 ps, and the "biological water" after considering the effects of both water and macromolecule dynamics at a timescale of *ca.* 10–20 ps, are well studied [49]. In particular, the ultrafast hydration dynamics in LCPs by time-resolved fluorescence spectroscopy using amino acid tryptophan-alkyl ester probes, three distinct timescales of water measured by relaxation dynamics were identified: (1) bulk water near the centre of the channel, (2) water layers adjacent to the lipid interface associated with a relaxation dynamics timescale *ca.* 10–15 ps, and (3) well-ordered interfacial water at the lipid surface with a timescale *ca.* 100–150 ps. In addition to the well understood bulk-like water at the centre of channels, categorically different residence times of water molecules in proximity to the lipid-water interface were observed by 2D NOESY, with water molecules near the MO glycerol moiety exhibiting effective residence time near to 380 ps, a measure of the translational diffusion properties of both lipid and water molecules.

A schematic representation of dynamic properties of water in terms of residence time in LCPs based on the present observations is shown in Fig. 8. Notably, an apparent increase in water residence time with sample age, as well as in the presence of cholesterol, is evident by 2D NOESY NMR spectroscopy. 2D NOESY and ROESY spectra of LCPs provide experimental validation of water residence time in proximity to MO in LCPs in order of tens to hundreds of ps. As expected, water in proximity to the glycerol moiety of MO exhibits a faster residence time compared to those further from the water channel. The potential for studying water dynamics in LCPs by spin–spin cross-relaxation based NMR techniques would be further enhanced if isotope-enriched lipids were readily available and, thus, heteronuclear NOE (HOESY) could be applied [50,51].

4. Conclusion

In the present study, 2D NOESY NMR spectroscopy was used to investigate the dynamic properties of water within lyotropic bicontinuous lipidic cubic phases (LCPs) composed of monoolein (MO). This approach yielded several novel observations regarding the hydration dynamics of these nanostructured lipid-water systems, illustrating the valuable role of this spectroscopic technique in lipid nanomaterial research.

Firstly, the effective residence time of water molecules in proximity to the glycerol headgroup has been categorically differentiated experimentally from those near the hydrophobic tail. Furthermore, 2D ^{1}H–^{1}H NOESY data have demonstrated an increase in effective residence time

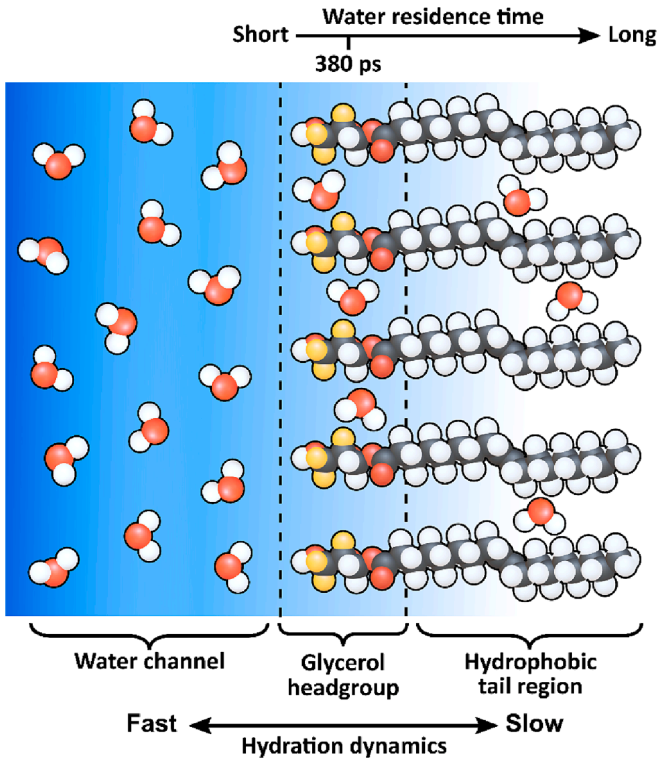

Fig. 8. A schematic representation of water dynamic properties in LCPs as revealed by 2D ^{1}H–^{1}H NOE NMR spectroscopy.

of water in proximity to the glycerol moiety of MO in LCPs, a phenomenon that became more pronounced as the sample aged, and with the introduction of an additive lipid, cholesterol. Possible explanations for these findings include modulation of lipid packing and organization, and subsequent changes to hydrogen bonding networks at the lipid-water interface influencing water dynamics in this region.

The analysis of cross-relaxation rates, derived from NOE build-up curves for water and the non-exchangeable protons of MO, has enhanced our understanding of the distribution and mobility of water in LCP systems. This technique opens new possibilities for investigating small molecules encapsulated within LCPs. Building on existing NMR studies of composition, structure, hydrocarbon chain dynamics and translational diffusion [39,52,53], our findings provide new insight into the properties of water in LCPs, and demonstrate an additional avenue using 2D NOE NMR spectroscopy for the study of water–lipid contact/hydration dynamics in lipid self-assemblies and nanomaterials.

2D ^{1}H–^{1}H NOESY/ROESY NMR spectroscopy provides a means for the quantitation of intermolecular cross-relaxation between water and individual spins of lipid molecules in LCPs. Hydration dynamics of other lipid self-assemblies, such as planar lipid bilayers or nanoparticles, could also be studied to further explore the lifetime of water molecules at the interface. Finally, detailed NOE NMR spectroscopic investigations of lipid membranes, both with and without cholesterol, could provide additional insights into the role of cholesterol in hydration dynamics within lipid membranes, with significant implications for our understanding of biological processes and the design of lipid nanomaterials [54].

CRediT authorship contribution statement

Thomas G. Meikle: Writing – review & editing, Writing – original draft, Visualization, Investigation, Conceptualization. **David W. Keizer:** Writing – review & editing, Investigation, Conceptualization. **Frances Separovic:** Writing – review & editing, Conceptualization. **Shenggen Yao:** Writing – review & editing, Writing – original draft, Visualization, Methodology, Investigation, Conceptualization.

Declaration of competing interest

The authors declare that they have no known competing financial interests or personal relationships that could have appeared to influence the work reported in this paper.

Data availability

Data will be made available on request.

Acknowledgments

The authors acknowledge support from and use of the Melbourne Magnetic Resonance platform, Bio21 Institute, University of Melbourne. S.Y. thanks Dr Marc-Antoine Sani (University of Melbourne) for discussions.

References

[1] S.K. Pal, A.H. Zewail, Dynamics of water in biological recognition, Chem. Rev. 104 (4) (2004) 2099–2123.
[2] S.S. Ribeiro, N. Samanta, S. Ebbinghaus, J.C. Marco, The synergic effect of water and biomolecules in intracellular phase separation, Nat. Rev. Chem. 3 (9) (2019) 552–561.
[3] J. Kim, W.Y. Lu, W.H. Qiu, L.J. Wang, M. Caffrey, D.P. Zhong, Ultrafast hydration dynamics in the lipidic cubic phase: discrete water structures in nanochannels, J. Phys. Chem. B 110 (43) (2006) 21994–22000.
[4] D.M. Mittleman, M.C. Nuss, V.L. Colvin, Terahertz spectroscopy of water in inverse micelles, Chem. Phys. Lett. 275 (3–4) (1997) 332–338.
[5] M.R. Harpham, B.M. Ladanyi, N.E. Levinger, K.W. Herwig, Water motion in reverse micelles studied by quasielastic neutron scattering and molecular dynamics simulations, J. Chem. Phys. 121 (16) (2004) 7855–7868.
[6] J.X. Cheng, S. Pautot, D.A. Weitz, X.S. Xie, Ordering of water molecules between phospholipid bilayers visualized by coherent anti-Stokes Raman scattering microscopy, Proceedings of the National Academy of Sciences 100 (17) (2003) 9826–9830.
[7] E.M. Landau, J.P. Rosenbusch, Lipidic cubic phases: a novel concept for the crystallization of membrane proteins, Proceedings of the National Academy of Sciences 93 (25) (1996) 14532–14535.
[8] V. Cherezov, J. Clogston, M.Z. Papiz, M. Caffrey, Room to move: crystallizing membrane proteins in swollen lipidic mesophases, J. Mol. Biol. 357 (5) (2006) 1605–1618.
[9] D.J. McClements, Encapsulation, protection, and release of hydrophilic active components: Potential and limitations of colloidal delivery systems, Advances in colloid and interface science 219 (2015) 27–53.
[10] S. Assenza, R.J.N.R.P. Mezzenga, Soft Condensed Matter Physics of Foods and Macronutrients, Nat. Rev. Phys. 1 (9) (2019) 551–566.
[11] H.M. Barriga, M.N. Holme, M.M. Stevens, Cubosomes: the next Generation of Smart Lipid Nanoparticles? Angew. Chem. Int. Ed. 58 (10) (2019) 2958–2978.
[12] Y. Yao, S. Catalini, B. Kutus, J. Hunger, P. Foggi, R. Mezzenga, Probing water state during lipidic mesophases phase transitions, Angew. Chem. Int. Ed. 60 (48) (2021) 25274–25280.
[13] J.J. Vallooran, S. Assenza, R.J.A.C. Mezzenga, Spatiotemporal Control of Enzyme-Induced Crystallization under Lyotropic Liquid Crystal Nanoconfinement. 131 (22) (2019) 7367–7371.
[14] T.P. Pitner, J.D. Glickson, J. Dadok, G.R. Marshall, Solvent exposure of specific nuclei of angiotensin-ii determined by Nmr solvent saturation method, Nature 250 (5467) (1974) 582–584.
[15] G. Otting, E. Liepinsh, K. Wuthrich, Protein hydration in aqueous-solution, Science 254 (5034) (1991) 974–980.
[16] D. Huster, K. Arnold, K. Gawrisch, Investigation of lipid organization in biological membranes by two-dimensional nuclear overhauser enhancement spectroscopy, J. Phys. Chem. B 103 (1) (1999) 243–251.
[17] D. Huster, K. Gawrisch, NOESY NMR crosspeaks between lipid headgroups and hydrocarbon chains: spin diffusion or molecular disorder? J. Am. Chem. Soc. 121 (9) (1999) 1992–1993.
[18] Y.Y. Cheng, Y.W. Li, Q.L. Wu, T.W. Xu, New insights into the interactions between dendrimers and surfactants by two dimensional NOE NMR spectroscopy, J. Phys. Chem. B 112 (40) (2008) 12674–12680.
[19] Y. Lingscheid, M. Paul, A. Brohl, J.M. Neudorfl, R. Giernoth, Determination of inter-ionic and intra-ionic interactions in a monofluorinated imidazolium ionic liquid by a combination of X-ray crystallography and NOE NMR spectroscopy, Magn. Reson. Chem. 56 (2) (2018) 80–85.
[20] P.A. Martin, F.F. Chen, M. Forsyth, M. Deschamps, L.A. O'Dell, Correlating Intermolecular cross-relaxation rates with distances and coordination numbers in Ionic liquids, J. Phys. Chem. Lett. 9 (24) (2018) 7072–7078.

[21] K. Gawrisch, H.C. Gaede, M. Mihailescu, S.H. White, Hydration of POPC bilayers studied by ¹H-PFG-MAS-NOESY and neutron diffraction, Eur. Biophys. J. Biophys. Lett. 36 (4–5) (2007) 281–291.
[22] A. Pampel, E. Strandberg, G. Lindblom, F. Volke, High-resolution NMR on cubic lyotropic liquid crystalline phases, Chem. Phys. Lett. 287 (3–4) (1998) 468–474.
[23] Y. Lu, D. Zhu, Q.Y. Le, Y.J. Wang, W. Wang, An NMR study on hydration and Molecular Interaction of phytantriol-based liquid crystals, Pharmaceutics 14 (11) (2022).
[24] M. Caffrey, D. Li, A. Dukkipati, Membrane protein structure determination using crystallography and lipidic mesophases: recent advances and successes, Biochemistry 51 (32) (2012) 6266–6288.
[25] T.G. Meikle, D.W. Keizer, J.J. Babon, C.J. Drummond, F. Separovic, C.E. Conn, S. Yao, Physiochemical Characterization and stability of lipidic cubic phases by solution NMR, Langmuir 36 (22) (2020) 6254–6260.
[26] R.E. Klevit, Improving two-dimensional Nmr-spectra by T1 ridge Subtraction, J. Magn. Reson. 62 (3) (1985) 551–555.
[27] S. Glaser, H.R. Kalbitzer, Improvement of two-dimensional Nmr-spectra by weighted mean T1-ridge Subtraction and antidiagonal reduction, J. Magn. Reson. 68 (2) (1986) 350–354.
[28] E. Veroutis, S. Merz, R.A. Eichel, J. Granwehr, Intra- and inter-molecular interactions in choline-based ionic liquids studied by 1D and 2D NMR, J. Mol. Liq. 322 (2021).
[29] J.M. Gruschus, J.A. Ferretti, Quantitative measurement of water diffusion lifetimes at a protein/DNA interface by NMR, J. Biomol. NMR 20 (2) (2001) 111–126.
[30] G. Otting, NMR studies of water bound to biological molecules, Prog Nucl Mag Res Sp 31 (1997) 259–285.
[31] S. Macura, R.R. Ernst, Elucidation of cross relaxation in liquids by two-dimensional Nmr-spectroscopy, Mol. Phys. 41 (1) (1980) 95–117.
[32] S. Macura, B.T. Farmer, L.R. Brown, An improved method for the determination of cross-relaxation rates from noe data, J. Magn. Reson. 70 (3) (1986) 493–499.
[33] T. Brand, E.J. Cabrita, S. Berger, Intermolecular interaction as investigated by NOE and diffusion studies, Prog Nucl Mag Res Sp 46 (4) (2005) 159–196.
[34] P. Honegger, M.E. Di Pietro, F. Castiglione, C. Vaccarini, A. Quant, O. Steinhauser, C. Schroder, A. Mele, The Intermolecular NOE depends on isotope selection: short range vs long range behavior, J. Phys. Chem. Lett. 12 (35) (2021) 8658–8663.
[35] H. Qiu, M. Caffrey, The phase diagram of the monoolein/water system: metastability and equilibrium aspects, Biomaterials 21 (3) (2000) 223–234.
[36] J. Briggs, M. Caffrey, The temperature-composition phase diagram of monomyristolein in water: equilibrium and metastability aspects, Biophysical journal 66 (3) (1994) 573–587.
[37] D.L. Gater, V. Reat, G. Czaplicki, O. Saurel, A. Milon, F. Jolibois, V. Cherezov, Hydrogen bonding of cholesterol in the lipidic cubic phase, Langmuir 29 (25) (2013) 8031–8038.
[38] P.O. Eriksson, G. Lindblom, Lipid and water diffusion in bicontinuous cubic phases measured by NMR, Biophys. J . 64 (1) (1993) 129–136.
[39] T.G. Meikle, D.W. Keizer, F. Separovic, S. Yao, A solution NMR view of lipidic cubic phases: structure, dynamics, and beyond, BBA Adv 2 (2022) 100062.
[40] C.Y. Cheng, L.L.C. Olijve, R. Kausik, S.G. Han, Cholesterol enhances surface water diffusion of phospholipid bilayers, J. Chem. Phys. 141 (22) (2014).
[41] S. Pyne, P. Pyne, R.K. Mitra, Addition of cholesterol alters the hydration at the surface of model lipids: a spectroscopic investigation, PCCP 24 (34) (2022) 20381–20389.
[42] M.D. Elola, J. Rodriguez, Influence of cholesterol on the dynamics of hydration in phospholipid bilayers, J. Phys. Chem. B 122 (22) (2018) 5897–5907.
[43] M.I. Oh, C.I. Oh, D.F. Weaver, Effect of cholesterol on the structure of networked water at the Surface of a model lipid membrane, J. Phys. Chem. B 124 (18) (2020) 3686–3694.
[44] K. Modig, E. Liepinsh, G. Otting, B. Halle, Dynamics of protein and peptide hydration, J. Am. Chem. Soc. 126 (1) (2004) 102–114.
[45] N.V. Nucci, M.S. Pometun, A.J. Wand, Site-resolved measurement of water-protein interactions by solution NMR, Nat. Struct. Mol. Biol. 18 (2) (2011) 245–U315.
[46] N.V. Nucci, M.S. Pometun, A.J. Wand, Mapping the hydration dynamics of ubiquitin, J. Am. Chem. Soc. 133 (32) (2011) 12326–12329.
[47] N.V. Nucci, K.G. Valentine, A.J. Wand, High-resolution NMR spectroscopy of encapsulated proteins dissolved in low-viscosity fluids, J. Magn. Reson. 241 (2014) 137–147.
[48] T.G. Meikle, A. Sethi, D.W. Keizer, J.J. Babon, F. Separovic, P.R. Gooley, C.E. Conn, S.G. Yao, Heteronuclear NMR spectroscopy of proteins encapsulated in cubic phase lipids, J. Magn. Reson. 305 (2019) 146–151.
[49] S.M. Cao, H.Y. Li, Z.N. Zhao, S.J. Zhang, J.Q. Chen, J.H. Xu, J.R. Knutson, L. Brand, Ultrafast fluorescence spectroscopy via upconversion and its applications in biophysics, Molecules 26 (1) (2021).
[50] L. Nordstierna, P.V. Yushmanov, I. Furo, Solute-solvent contact by intermolecular cross relaxation. I. the nature of the water-hydrophobic interface, J. Chem. Phys. 125 (7) (2006).
[51] L. Nordstierna, P.V. Yushmanov, I. Furo, Solute-solvent contact by intermolecular cross-relaxation. 2. the water-micelle interface and the micellar interior, J. Phys. Chem. B 110 (51) (2006) 25775–25781.
[52] G. Lindblom, G. Oradd, Nmr-studies of translational diffusion in lyotropic liquid-crystals and lipid-membranes, Prog Nucl Mag Res Sp 26 (1994) 483–515.
[53] S. Yao, T.G. Meikle, F. Separovic, D.W. Keizer, Recent studies of lyotropic lipidic cubic phases, in: W.S. Price (Ed.), *Annual Reports on NMR Spectroscopy* 110, Elsevier, 2023, pp. 31–78.
[54] E. Ikonen, Cellular cholesterol trafficking and compartmentalization, Nat. Rev. Mol. Cell Biol. 9 (2) (2008) 125–138.